On the Graphical Representation of Electric Field Lines in Waveguide

PAUL E. MOLLER, MEMBER, IEEE, AND ROBERT H. MACPHIE, SENIOR MEMBER, IEEE

Abstract — **A method is presented for illustrating the time-varying behavior of electric field lines in the neighborhood of a parallel-plate waveguide E-plane step discontinuity. Sequences of electric field plots illustrating the time-varying behavior for several E-plane step heights are included. The method presented is applicable to analogous junctions in rectangular waveguide and can be extended to more complex waveguide structures.**

I. Introduction

THE PLOTTING of electrostatic field lines and potentials in the neighborhood of charged conductors has had a long history. Indeed one must look hard to find more interesting and elegant field plots than those to be found at the end of Volume I of Maxwell's famous treatise [1] which first appeared over one hundred years ago. Moreover, two-dimensional field plots for a wide variety of configurations have been achieved by conformal mapping techniques [2], [3, ch. 6]. In addition, the well-known scheme of solving Laplace's equation by the method of curvilinear squares is routinely presented in many undergraduate textbooks [4], [5].

The more difficult problem of obtaining a graphical representation of solutions to the Helmholtz equation, and in particular field plots in waveguide, has also occupied the attention of many workers. Most text books [6], [7] illustrate the lines of the electric and magnetic fields of the lower order modes in rectangular and circular waveguide. In the *Waveguide Handbook* [7], one finds some good illustrations of the fields in coaxial and elliptical waveguides as well.

With the advent of the large digital computer, numerical techniques became very popular. Beaubien and Wexler [8] used the *finite-difference method* to obtain cross-sectional contour plots of constant E_z and constant H_z (TM and TE modes) for rectangular, circular, ridge, and lunar waveguides. Using the *finite-element method*, Silvester [9] showed that similar contour plots could be generated. Later, some very fine contour plots of E_z and H_z in dielectric-loaded waveguide appeared in a paper by Csendes and Silvester [10] and at the same time Beaubien and Wexler [11] presented an improved finite-difference method, with numerous cross-sectional contour plots of E_z and H_z in a variety of guides, including a T-septate guide.

In some recent papers, the conservation of complex power techniques has been used to solve some problems involving the junctions of parallel plate [12], [13] and rectangular [14] waveguides. In particular, if a single dominant mode is incident from one of the waveguides, the technique provides the amplitudes and phases of all scattered modes and, in principle, is exact; however, in the numerical solutions, a finite number of modes are sufficient to provide a satisfactory representation of the total electromagnetic field in the neighborhood of the junction.

Using the modal series expansions (TM modes only) for the fields on either side of an E-plane step junction of two parallel-plate waveguides, this paper presents a technique for plotting the lines (in the sense of Faraday) of the real instantaneous electric field in the neighborhood of the junction. A single TEM wave is assumed to be incident from the smaller of the two guides. The plots are in the yz plane containing the guide axis rather than in the xy (transverse plane). Moreover, they represent the vector E-field $\bar{E}_{yz}$ rather than contour plots of E_z as in [8]–[11].

II. Normal Mode Expansion of Waveguide Fields

Let us assume that the waveguide electric fields are known in terms of an expansion series of normal modes [12], [13]. In this paper, we will be considering parallel-plate waveguides, with attention being given to the dynamic field behavior in the neighborhood of E-plane steps connecting two waveguides (refer to Fig. 1) when there is a dominant TM_0 mode wave incident on the junction from the smaller of the two guides.

Accordingly, it is easy to show that the y and z components of the real instantaneous TM fields are as follows:

$$\mathscr{E}_{1y}(y,z,t) = \cos(\omega t - k_0 z) + a_0 \cos(\omega t + k_0 z + \phi_0) + \sum_{\substack{m=2 \\ m \text{ even}}}^{\infty} a_m \cos\left(\frac{m\pi}{b_1} y\right) e^{\alpha_{1m} z} \cos(\omega t + \phi_m) \quad (1)$$

$$\mathscr{E}_{1z}(y,z,t) = \sum_{\substack{m=2 \\ m \text{ even}}}^{\infty} a_m \frac{m\pi}{\alpha_{1m} b_{1m}} \sin\left(\frac{m\pi}{b_1} y\right) \cdot e^{\alpha_{1m} z} \cos(\omega t + \phi_m), \qquad 0 \leqslant |y| \leqslant b/2,\ z < 0. \quad (2)$$

In (1) and (2), ω is the operating frequency and c is the

Manuscript received August 3, 1983; revised September 30, 1984. This work was supported in part by the Natural Sciences and Engineering Research Council, Ottawa, under Grant A 2176.

P. E. Moller is with the Telecommunication Services Engineering, Telesat Canada, Ottawa, Ontario, Canada KIL 8B9

R. H. MacPhie is with the Electrical Engineering Department, University of Waterloo, Waterloo, Ontario, Canada N2L 3G1

0018-9480/85/0300-0187$01.00 ©1985 IEEE

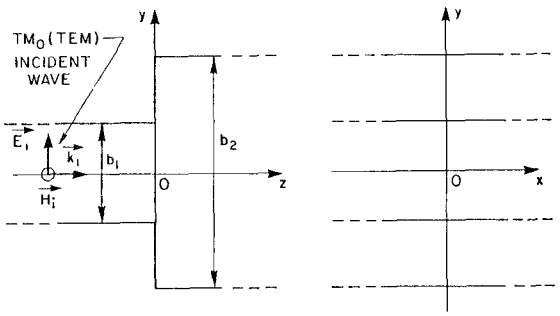

Fig. 1. Parallel-plate waveguide junction with E-plane step discontinuity.

velocity of light; then

$$k_0 = \frac{\omega}{c}, \quad \alpha_{1m} = \sqrt{\left(\frac{m\pi}{b_1}\right)^2 - k_0^2} \geq 0. \tag{3}$$

The incident TEM mode's amplitude is unity and $a_m e^{j\phi_m}$ is the complex amplitude of the mth reflected mode, $m = 0,2,4, \cdots$. It is assumed that only the TEM mode ($m = 0$) can propagate.

On the other side of the junction ($z = 0$), the fields are

$$\mathscr{E}_{2y}(y,z,t) = b_0 \cos(\omega t - k_0 z + \theta_0) + \sum_{\substack{n=2 \\ n \text{ even}}}^{\infty} b_n \cos\left(\frac{n\pi}{b_2} y\right) e^{-\alpha_{2n} z} \cos(\omega t + \theta_n) \tag{4}$$

$$\mathscr{E}_{2z}(y,z,t) = \sum_{\substack{n=2 \\ n \text{ even}}}^{\infty} b_n \frac{n\pi}{\alpha_{2n} b_2} \sin\left(\frac{n\pi}{b_2} y\right) e^{-\alpha_{2n} z} \cos(\omega t + \theta_n), \quad |y| \leq b_2/2, z > 0 \tag{5}$$

and where

$$\alpha_{2n} = \sqrt{\left(\frac{n\pi}{b_2}\right)^2 - k_0^2}. \tag{6}$$

In (4) and (5), $b_n e^{j\theta_n}$ is the complex amplitude of the nth transmitted mode, $n = 0,2,4, \cdots$. Both m and n are even due to the even symmetry of the junction and the TEM excitation.

III. Representation of the Electric Field Lines

We follow the traditional definition of electric field lines. The tangent vector at any point on a curvilinear electric field line is in the direction of the electric field strength $\vec{\mathscr{E}}$ at that point and the density of lines in the neighborhood of the point is proportional to $|\vec{\mathscr{E}}|$.

Each electric field line is approximated by a sequence of line segments of equal length, the first of which is at a plane of symmetry in the waveguide which is the central plane $y = 0$, as indicated in Fig. 1. The initial line segments are perpendicular to this plane; physically it is equivalent to an electric wall with the normal E-field proportional to the surface electric charge density

$$\epsilon_0 \mathscr{E}_y(0,z,t) = \sigma_s. \tag{7}$$

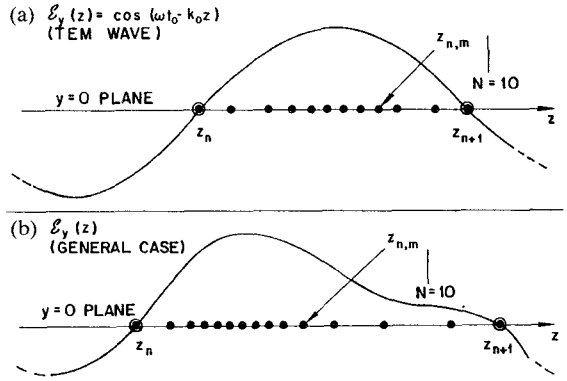

Fig. 2. (a) Distribution of electric field line starting points for a single TEM wave. (b) Distribution of electric field line starting points for a general field.

Moreover, the problem of scattering by an asymmetric E-plane step in which the bottom wall of each waveguide is at $y = 0$ has the same solution as that in the upper half of the symmetric structure. In the former case, the initial line segments are at the surface of the bottom wall, perpendicular to it, and with a density proportional to σ_s.

IV. Calculation of the Starting Points

The starting points of the initial line segments can be regarded as being at the surface charges (equivalent or actual) on the plane $y = 0$; the charge density is proportional to $\mathscr{E}_y(0,z,t)$. Consequently, for any fixed time, say $t = t_0$, the normal E-field at $y = 0$ is a *known* function of z (given by (1) and (4) with $y = 0$). In Fig. 2(a) is a graph of the field when there is only a single positively traveling wave ($a_m = 0$, $m = 0,2,4, \cdots$) and Fig. 2(b) illustrates a more general distribution of $\mathscr{E}_y$.

In the quasi-trivial case of Fig. 2(a), we specify the total number of lines N associated with each half cycle of the wave; in usual practice, $10 \leq N < 50$, with the computer time to plot the field lines increasing linearly with N. Next, we locate the nulls of $\mathscr{E}_y$ in the range of interest $z_{\min} < z < z_{\max}$. Let z_n be the nth such null with $z_0 < z_{\min} < z_1 < z_2 < \cdots < z_n < \cdots < z_{\max} < z_{Q+1}$.

In any half wavelength interval, say $z_n < z < z_{n+1}$, the N lines of the electric field start at points $z_{n,m}$ and are located at the centers of sub-intervals. The integral of $\mathscr{E}_y$ (surface charge) over each sub-interval is $(1/N)$th of the total integral (surface charge) between nulls. It follows that the mth line's starting point is

$$z_{n,m} = \tfrac{1}{2}(\tilde{z}_{n,m+1} + \tilde{z}_{n,m}) \tag{8}$$

where

$$m = \frac{k_0 N}{2} \int_{\tilde{z}_{n,1}}^{\tilde{z}_{n,m+1}} \cos(\omega t_0 - k_0 z)\, dz \tag{9}$$

with $m = 1,2,\cdots,N-1$, and $\tilde{z}_{n,1} = z_n$. It is straightforward to show that for the single positively traveling TEM wave

$$\tilde{z}_{n,m+1} = z_n + \frac{\cos^{-1}\left(1 - \frac{2m}{N}\right)}{2\pi} \lambda_0 \tag{10}$$

where λ_0 is the TEM mode's wavelength.

In the general case where the field $\mathscr{E}_y$ involves higher order modes, it is still possible to determine the nulls numerically by means of the modal series expansions and a standard zero finding routine. However, the integral of $\mathscr{E}_y$ between any two successive nulls, say z_n and z_{n+1}, will in general not correspond to an *integer number* of lines N_n. Accordingly, for the general case, (9) is replaced by

$$m = T_n \frac{k_0 N}{2} \int_{z_n}^{z_{n,m+1}} \mathscr{E}_y \, dz, \qquad m = 1, 2, 3, \cdots, N_n - 1. \tag{11}$$

In (11), T_n the "tweaking" factor is defined as

$$T_n = \frac{\text{Integer}\left[\frac{k_0 N}{2} \int_{z_n}^{z_{n+1}} \mathscr{E}_y \, dz\right]}{\frac{k_0 N}{2} \int_{z_n}^{z_{n+1}} \mathscr{E}_y \, dz} = \frac{N_n}{\frac{k_0 N}{2} \int_{z_n}^{z_{n+1}} \mathscr{E}_y \, dz}. \tag{12}$$

In (12), Integer[x] indicates the integer nearest x. Thus, the "tweaking" factor adjusts the overall strength of $\mathscr{E}_y$ so that an integer number of lines will be located between each pair of nulls, an obviously necessary graphical constraint. The integration in (11) and (12) is performed numerically in the general case due to the large number of modes involved.

V. Sequential Plotting of the Electric Field Line Segments

Due to the even symmetry of the electric field $\vec{\mathscr{E}}(y, z, t)$ about the center line $y = 0$, we will describe the plotting procedure only for the $y > 0$ region. From each starting point $z_{n,m}$ on the $y = 0$ axis of symmetry, a perpendicular line segment of length Δ is drawn (see Fig. 3). Its end point is ($y = \Delta$, $z = z_{n,m}$). The segment length is normally between one tenth and one fiftieth of the height of the waveguide with plotting time inversely proportional to Δ.

The second and subsequent line segments, but not the last, are determined according to the following scheme.

a) Let θ_{i-l} be the direction of the $(i-l)$th line segment and its end point be at $p_{i-l}^{+} = (y_{i-l}^{+}, z_{i-l}^{+})$.

b) The initial direction of the ith line segment is taken to be the same as that of the $(i-l)$th segment.

c) In the angular interval $\pm \Delta\theta$, centered on the initial direction θ_{i-l}, the *geometrical slope* of a line segment with starting point p_{i-l}^{+} and angle $\tilde{\theta}_i = \theta_{i-l} + \delta\theta_i$ is simply

$$S_{g,i}(\tilde{\theta}_i) = \frac{\Delta y_i}{\Delta z_i} = \tan(\tilde{\theta}_i). \tag{13}$$

The slope of the electric field vector at the midpoint of the same line segment is

$$S_{ef,i}(\tilde{\theta}_i) = \frac{\mathscr{E}_y\left[y_{i-l}^{+} + \frac{\Delta}{2}\sin(\tilde{\theta}_i),\ z_{i-l}^{+} + \frac{\Delta}{2}\cos(\tilde{\theta}_i),\ t\right]}{\mathscr{E}_z\left[y_{i-l}^{+} + \frac{\Delta}{2}\sin(\tilde{\theta}_i),\ z_{i-l}^{+} + \frac{\Delta}{2}\cos(\tilde{\theta}_i),\ t\right]}. \tag{14}$$

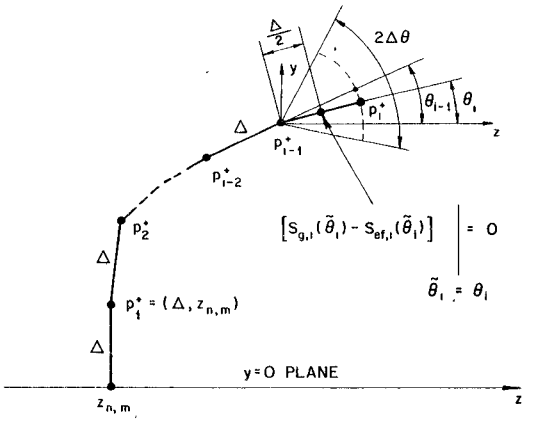

Fig. 3. Angular relations in the construction of the ith segment of an electric field line.

d) The angle $\tilde{\theta}_i$ is then varied until

$$\left[S_{g,i}(\tilde{\theta}_i) - S_{ef,i}(\tilde{\theta}_i)\right]\Big|_{\tilde{\theta}_i = \theta_i} = 0 \tag{15}$$

where θ_i is the angle of the ith line segment whose slope is equal to the slope of the E-field at its midpoint. This is accomplished numerically by using (13) and (15) together with a suitable zero finding routine on a digital computer. The angular interval $2\Delta\theta$ over which the zero of (15) is sought is taken to be equal to or less than 90° in practice.

It is also convenient to avoid the case when the slopes given by (13) and (14) become very large ($\tilde{\theta}_i = \pm 90°$). This can be done by matching *inverse slopes*, easily derived from (13)–(15). Indeed, if $|\theta_{i-l}| > 45°$, then we use the inverse slope formulation for θ_i, and if $|\theta_{i-l}| < 45°$, the slope equations are employed.

VI. Terminating the Lines

The sequence of line segments representing a particular line of electric field will eventually approach the conducting waveguide top wall or curve back to the center line at $y = 0$ or perhaps simply pass beyond the interval $[z_{\min}, z_{\max}]$ in which we are interested in a field plot. Fig. 4 indicates the eight distinct terminating regions for our particular problem.

In the plotting sequence, each line segment's end point p_n^{+} is monitored to check if it has fallen into any terminating region. If it hasn't, the plotting continues; if it has, the next line is a terminating line whose direction is dictated by the nature of the region, with, for example, a perpendicular segment joining p_i^{+} to any nearby conducting waveguide wall or in our case to the center line $y = 0$. For region 2, the terminating line joins p_i^{+} to the corner point at $y = b_1/2$, $z = 0$.

VII. The Electric Field Line Plots

The plotting methods described in Sections IV–VI were implemented on a digital computer (IBM 4341) in Fortran code. Plots of the field lines were then produced with a Zeta 3653 SX drum plotter.

Let us first consider the *asymmetric case* where $y = 0$ is the lower wall of the waveguide structure and the upper

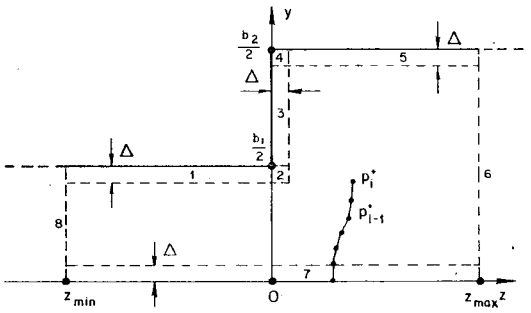

Fig. 4. Terminating regions for the single E-plane step discontinuity in waveguide.

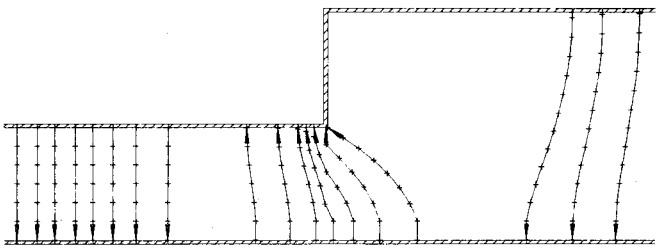

Fig. 5. Electric field lines at an asymmetric 1:2 E-plane step discontinuity in parallel-plate waveguide with a TEM wave incident from the smaller guide; $b_2/2 = b_1 = 0.4\ \lambda_0$, $t = 0$, $N = 8$, $\Delta = b_1/6$, $|z| \leqslant \lambda_0/2$.

walls of the two parallel-plate guides are at

$$y = 0.2\lambda_0 = \frac{b_1}{2} \text{ and } y = 0.4\lambda_0 = \frac{b_2}{2}.$$

Let $N = 8$ and $\Delta = b_1/6$, a rather coarse representation which clearly illustrates the principle of the line segment method of field plotting. Fig. 5 gives the resulting plot for the interval $|z| \leqslant \lambda_0/2$ and for $t_0 = 0$, the instant at which the crest of the incident TEM wave is striking the junction at $z = 0$. The ends of line segments are marked by "+" signs. In the smaller guide, the field lines differ only slightly from the vertical lines of the TEM modes. This is due to the rapid attenuation of the higher order cutoff modes reflected from the junction. In the larger guide, this attenuation is considerably less and results in the field lines curving back to the top wall at $z = 0$. In this case, the higher order modes in the larger guide die out for practical purposes by $z = 0.50\ \lambda_0$, at which point there is only the TEM transmitted wave passing out of our region of interest. Accordingly, to save computation time, the maximum number of available modes are used to compute $\mathscr{E}_y$ and $\mathscr{E}_z$ in the immediate neighborhood of the discontinuity and progressively fewer are used as $|z|$ increases.

In the small guide at a particular value of $z < 0$, we employ the following criteria:

for $\mathscr{E}_x$, if $e^{\alpha_{1\tilde{m}}z} < \gamma$, $\tilde{m}$ is the highest order mode used,

for $\mathscr{E}_y$, if $e^{\alpha_{1\hat{m}}z} < \gamma\alpha_{1\hat{m}}$, $\hat{m}$ is the highest order mode used.

The factor γ is an arbitrary small number. In the large guide for a particular $z > 0$, we have the corresponding criteria:

for $\mathscr{E}_x$, if $e^{-\alpha_{2\tilde{n}}z} < |b_0|\gamma$, $\tilde{n}$ is the highest order mode used,

for $\mathscr{E}_y$, if $e^{-\alpha_{2\hat{n}}z} < |b_0|\gamma\alpha_{2\hat{n}}$,

$\hat{n}$ is the highest order mode used.

TABLE I
NUMBER OF MODES USED AS A FUNCTION OF DISTANCE FROM THE JUNCTION PLANE

$\lvert z\rvert/\lambda_0$	Small Guide		Large Guide	
0	24	24	48	48
0.10	18	14	44	32
0.25	8	8	16	14
0.50	6	6	10	8
0.75	4	4	8	6
1.00	4	4	6	6
$\gamma = 10^{-4}$	$\tilde{m}$	$\hat{m}$	$\tilde{n}$	$\hat{n}$

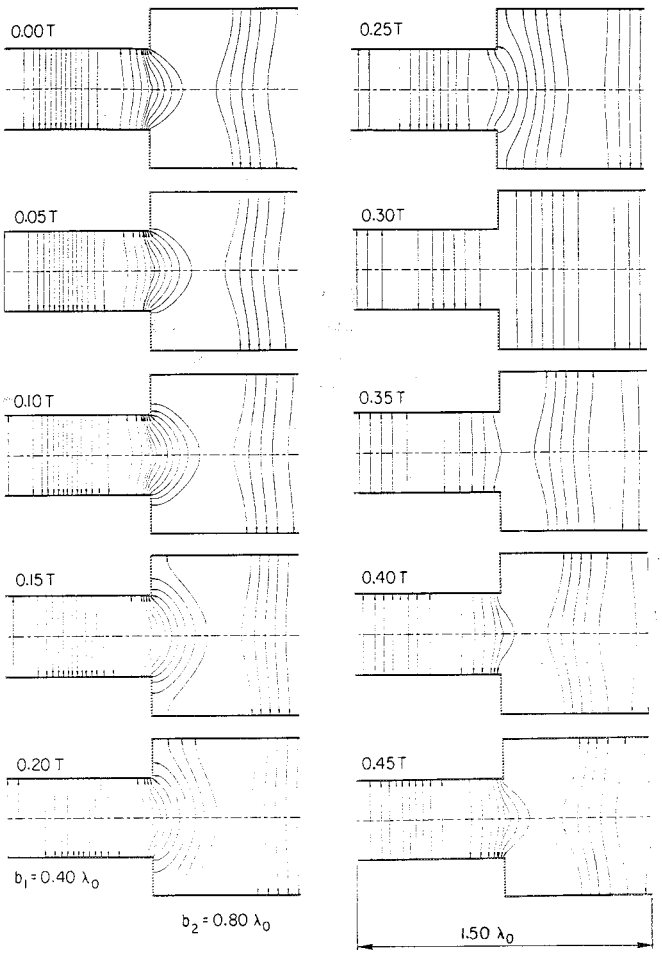

Fig. 6. Electric field lines at a symmetric 1:2 E-plane step discontinuity in parallel-plate waveguide with a TEM wave incident from the smaller guide; $b_2 = 2b_1 = 0.80\ \lambda_0$, $\Delta T = 0.05$ T, $N = 10$, $\Delta = b_1/33$.

$|b_0|$ is the amplitude of the dominant TEM mode scattered into the larger guide.

Table I indicates the number of modes used at various distances from the junction illustrated in Fig. 5, when the maximum number of available modes in the smaller and larger guides are, respectively, 12 ($m_{max} = 24$) and 24 ($n_{max} = 48$), and when $\gamma = 10^{-4}$.

Figs. 6–8 show field line plots for the case of symmetric junctions of parallel-plate waveguides (E-plane steps) when incidence is from the smaller (left) guide in the form of a TM_0 wave. In all cases, the number of lines per half

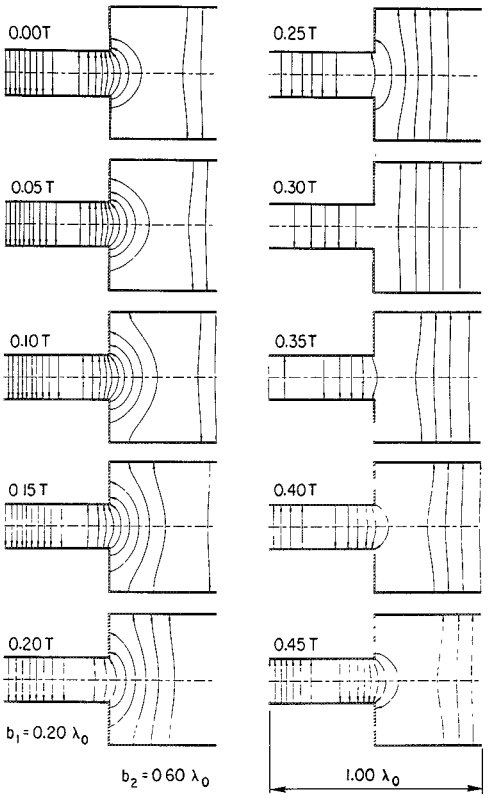

Fig. 7. Electric field lines at a symmetric 1:3 E-plane step discontinuity in parallel plate waveguide with a TEM wave incident from the smaller guide; $b_2 = 3b_1 = 0.60\ \lambda_0$, $\Delta T = 0.05$ T, $N = 10$, $\Delta = b_1/33$.

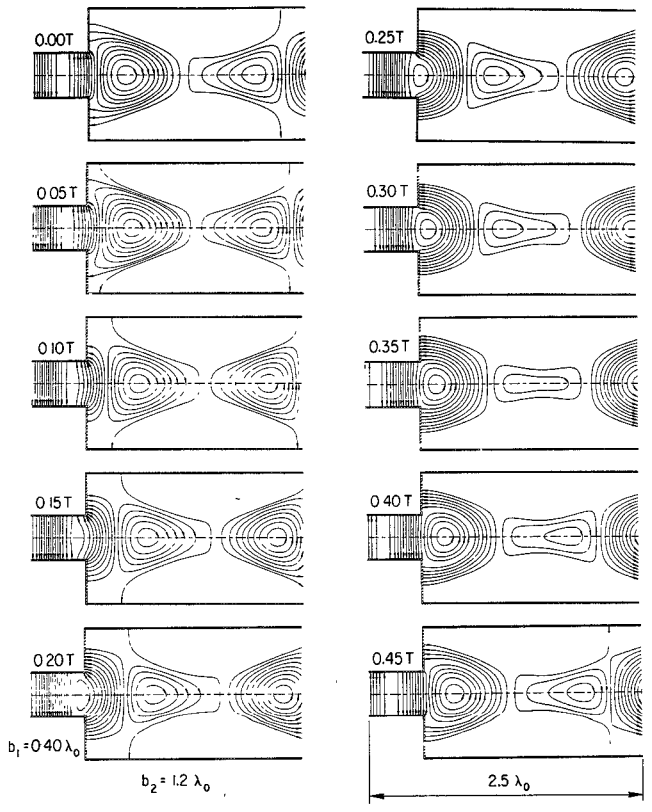

Fig. 8. Electric field lines at a symmetric 1:3 E-plane step discontinuity in parallel plate waveguide with a TEM wave incident from the smaller guide; $b_2 = 3b_1 = 1.20\ \lambda_0$, $\Delta T = 0.05$ T, $N = 10$, $\Delta = b_1/33$.

wavelength of the incident wave has been increased to $N = 10$ and the line segments decreased to $\Delta = b_1/33$. To illustrate the dynamic behavior of the scattering by such junctions, the first half of a period is covered in increments of $\Delta t = 0.05$ T from 0 to 0.45 T. The second half of the RF period yields identical plots except for a reversal of the lines of the E-field.

A 1:2 E-plane step with $b_1 = 0.4\ \lambda_0$ and $b_2 = 0.8\ \lambda_0$ is shown in Fig. 6. The crest of the incident wave appears at the junction at $t = 0.00$ T. Note the high E-field (density of lines) at the two 90° corners ($z = 0$, $y = \pm b_1/2$). This is expected since the edge condition [12, p. 341] dictates that $|\bar{E}|$ is proportional to $r^{-1/3}$, where r is the radial distance from the corner. As the crest of the TM_0 wave travels past the junction, the electric field lines can be seen terminating on the vertical walls. Finally, the electric field lines become nearly vertical as the higher order modes decay and the TM_0 mode again dominates. The number of electric field lines is reduced because, in this case, the TM_0 transmission coefficient magnitude is $|b_0| = 0.63$.

Fig. 7 shows a 1:3 E-plane step in which $b_1 = 0.2\ \lambda_0$ and $b_2 = 0.6\ \lambda_0$. The waveguide dimensions of Fig. 7 are smaller than that of Fig. 6 and thus the higher order modes die off faster. Whereas in Fig. 6 the higher order modes have mostly decayed by $z = 0.6\ \lambda_0$, in Fig. 7 the modes have mostly decayed by $z = 0.3\ \lambda_0$.

Fig. 8 shows a 1:3 E-plane step in which $b_1 = 0.4\ \lambda_0$ and $b_2 = 1.2\ \lambda_0$. The most interesting feature is the vortex of E-field lines closing on themselves (instead of on surface charge at $y = \pm b_2/2$). This is due to the interaction of the TEM (TM_0) mode and the TM_2 mode which for a guide height of 1.2 λ is a *propagating* mode. Its phase velocity is about 1.8 times the velocity of light and its amplitude is comparable to that of the TEM mode ($|b_2| = 0.51$, $|b_0| = 0.31$).

VIII. Discussion and Conclusions

This paper has illustrated the dynamic (time varying) behavior of electric field lines in the neighborhood of an E-plane step discontinuity in parallel-plate waveguide. The technique is exact in principle since plotting involves a complete set of TM modes, and the line density N and line segment length Δ are arbitrary. In our examples, about 24 modes in the smaller of the two waveguides, line densities of $N = 10$ per half wavelength of the incident wave, and line segments of $\Delta \simeq 3$ percent of the smaller height were used to yield the field line plots of Figs. 6–8.

In regard to computation and plotting times using the IBM 4341 computer and the Zeta 3653 SX drum plotter, the plot of Fig. 5 involved 50 s of time for mode coefficient generation (24 modes in the smaller guide and 48 in the larger) and about 80 s to calculate the electric field lines. Plotting of *each* of the ten plots in Figs. 6–8 took about 18 min, with each original hard copy plot being about 40 cm × 20 cm.

The sequence of images of $\bar{E}_{yz}$ in Figs. 6–8 suggests that one could make a moving picture with a sufficient number of such "cartoons." We have done so using $\Delta t = 0.25$ T

and 1:2 E plane step. The resulting "film", recorded on video tape, lasts about 110 s and corresponds to 16 periods of the RF field. The field lines move in somewhat jerky fashion but we are reasonably sure that if Δt were reduced to 0.0125 T and the time per period reduced to say 4 s, we could, with a resulting frame rate of 20 per second, achieve a very acceptable representation of the electric field lines' dynamic behavior.

Although used here for the quite simple configuration of an E-plane step in parallel-plate waveguide, this method is applicable to analogous junctions in rectangular waveguide [14]. In the near future, we are aiming at obtaining electric field line plots in the neighborhood of a thick diaphram with a circular iris located in rectangular waveguide. Later we hope to get plots for a resonator cavity made up of two such diaphrams in rectangular waveguide. Many other waveguide junctions can be considered.

References

[1] J. C. Maxwell, *Treatise on Electricity and Magnetism, 3rd Ed.* New York: Dover Publications, 1952.

[2] K. J. Binns and P. J. Lawrenson, *Analysis and Computation of Electric and Magnetic Field Problems*, Second Ed. Oxford, England: Pergamon Press, 1973.

[3] W. J. Gibbs, *Conformal Transformations in Electrical Engineering.* London: Chapman and Hall, 1958.

[4] C. R. Paul and S. A. Nasar, *Introduction to Electromagnetic Fields.* New York: McGraw-Hill, 1982.

[5] G. G. Skitek and S. V. Marshall, *Electromagnetic Concepts and Applications.* Englewood Cliffs, NJ: Prentice Hall, 1982.

[6] S. Ramo, J. R. Whinnery, and T. van Duzer, *Fields and Waves in Communication Electronics.* New York: Wiley, 1965.

[7] N. Marcuvitz, Ed., *Waveguide Handbook.* New York: Dover Publications, 1965.

[8] M. J. Beaubien and A. Wexler, "An accurate finite difference method for higher order waveguide modes," *IEEE Trans. Microwave Theory Tech.*, vol. MTT-16, pp. 1007–1017, Dec. 1968.

[9] P. Silvester, "Finite element solution of homogeneous waveguide problems," *Alta Frequenza*, vol. XXXVIII, N. Speciale, pp. 313–317, May 1969.

[10] Z. J. Csendes and P. Silvester, "Numerical solution of dielectric loaded waveguides: I—Finite-element analysis," *IEEE Trans. Microwave Theory Tech.*, vol. MTT-18, pp. 1124–1131, Dec. 1970.

[11] M. J. Beaubien and A. Wexler, "Unequal-arm finite-difference operators in the positive-definite successive over-relaxation (PDSOR) algorithm," *IEEE Trans. Microwave Theory Tech.*, vol. MTT-18, pp. 1132–1149, Dec. 1970.

[12] R. Safavi Naini and R. H. MacPhie, "On solving waveguide scattering problems by the conservation of complex power technique," *IEEE Trans. Microwave Theory Tech.*, vol. MTT-29, pp. 337–343, Apr. 1981.

[13] E. M. Sich and R. H. MacPhie, "The conservation of complex power technique and E-plane step-diaphragm junction discontinuities," *IEEE Trans. Microwave Theory Tech.*, vol. MTT-30, pp. 198–201, Feb. 1982.

[14] R. Safavi Naini and R. H. MacPhie, "Scattering at rectangular-to-rectangular waveguide junctions," *IEEE Trans. Microwave Theory Tech.*, vol. 30, pp. 2060–2063, Nov. 1982.

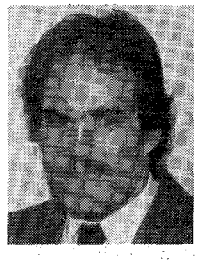

Paul E. Moller (S'80–M'82) was born in Montreal, Quebec, Canada, on July 12, 1958. He received the B.A.Sc. degree in electrical engineering from the University of Waterloo in 1982.

In 1982, he joined Telesat Canada, Ottawa, Ontario, Canada, as a Project Engineer. He developed ground communications equipment for a satellite space diversity system used in Canada's high Arctic. Mr. Moller has developed wide-band microwave circulators for communications satellites. His present interests include SAW devices, signal processing, and spread spectrum communication systems.

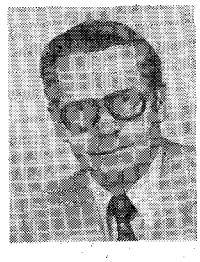

Robert H. MacPhie (S'57–M'63–SM'79) was born in Weston, Ontario, Canada, on September 20, 1934. After receiving the B.A.Sc. degree in electrical engineering from the University of Toronto in 1957, he earned the M.S. and Ph.D. degrees at the University of Illinois, Urbana, in 1959 and 1963, respectively.

In 1963, he joined the University of Waterloo, Waterloo, Ontario, Canada, as an Assistant Professor in Electrical Engineering and at present he is Professor of Electrical Engineering at Waterloo. His research interests currently focus on antenna arrays, waveguide scattering theory, scattering from prolate spheroid systems, and microstrip structures. During 1984–1985, he has been on sabbatical leave as a Professeur Associé at the University of Aix-Marseille I, France, working at the Laboratorie de Radioélectricité.